

# Fermi National Accelerator Laboratory

FERMILAB-Pub-84/36-E  
7320.401  
(Submitted to Phys. Rev. Lett.)

$\rho$  PHOTOPRODUCTION FROM 45 TO 225 GeV

P. Callahan, G. Gladding, C. Olszewski, and A. Wattenberg  
University of Illinois at Urbana-Champaign, Urbana, Illinois 61801

and

M. Binkley, J. Butler, J. P. Cumalat, I. Gaines, M. Gormley,  
D. J. Harding, R. L. Loveless, and J. Peoples  
Fermi National Accelerator Laboratory, Batavia, Illinois 60510

March 1984



$\rho$  Photoproduction from 45 to 225 Gev

P. Callahan<sup>(a)</sup>, G. Gladding, C. Olszewski, and A. Wattenberg

University of Illinois at Urbana-Champaign  
Urbana, Illinois 61801

M. Binkley, J. Butler, J. P. Cumalat<sup>(b)</sup>, I. Gaines, M. Gormley,  
D. J. Harding, R. L. Loveless<sup>(c)</sup>, and J. Peoples

Fermi National Accelerator Laboratory  
Batavia, Illinois 60510

Measurements of the energy and  $t$  dependence of diffractive  $\rho$  photoproduction are presented. The elastic  $\rho$  cross-section is approximately constant over the entire energy range at a value of  $10.0 \pm 0.1 \mu\text{b}$ . The  $t$  dependence of both the elastic and inelastic parts of diffractive  $\rho$  photoproduction are identical to those of diffractive pion production in  $\pi p$  interactions as predicted by the additive quark model.

Shortly after the discovery of the  $\rho$  meson in hadronic interactions<sup>1</sup>, the first measurements of the production of  $\rho$  mesons from hydrogen by photons of energy  $1 + 6$  Gev were made in 1964.<sup>2</sup> In the intervening years many experiments have been done, the results of which have formed the basis for the understanding of the hadronic properties of the photon in terms of vector meson dominance and additive quark models.<sup>3</sup> We present here extensive new measurements of the s and t dependence of the photoproduction of  $\rho$  mesons from hydrogen in the energy region of 45 to 225 Gev.

The data reported here were taken in the broadband photon beam at Fermilab. Both the beam and detector have been described elsewhere.<sup>4</sup> Briefly, particles produced with angles less than 35 mrad with respect to the photon beam were detected in a multiparticle spectrometer, consisting of two analyzing magnets, a multi-wire proportional chamber tracking system, two multicell Cherenkov counters with pion thresholds of 6 and 12 Gev, respectively, a fly's-eye array of lead-glass blocks, and a steel-scintillator hadron calorimeter. In addition, three concentric hexagonal scintillation counter arrays were positioned around the 41 cm liquid hydrogen target in order to detect target fragments. These rings provided azimuthal angle resolution of  $\pm 10^\circ$  for protons with momenta greater than 280 Mev/c.

Events were collected which satisfied a trigger formed from the information from scintillation counters, the multiwire proportional chambers, and the hadron calorimeter. In particular, the trigger counter and multiwire proportional chamber data were required to be consistent with the presence of at least 2 but not more than 8 charged tracks, and a minimum of 25 Gev was required to be deposited in the hadron calorimeter. The presence of the lead-glass in front of the hadron calorimeter and the limited resolution of the calorimeter itself combine to make this energy deposition requirement the

dominant contributor to the energy dependence of the acceptance. For example, the calorimeter acceptance rises from 33% at 45 Gev to 90% at 140 Gev.

The  $\rho$  analysis proceeded by first selecting events with exactly two reconstructed tracks of opposite charge which originate in the target. Information from the lead-glass array was then used to eliminate those events containing either reconstructed  $\pi^0$ 's or photons of energy 5 Gev or more. Events containing at least one track which was unambiguously identified as a kaon by the Cherenkov counter analysis were also removed from the sample. Finally, those events which were not consistent with the elastic reaction

$$\gamma + p \rightarrow \pi^+ + \pi^- + p, \quad (1)$$

as determined by the recoil detector analysis, were eliminated. The events cut by the elastic recoil requirement accounted for 27% of those events which passed all the previous cuts. We call these events "diffractive inelastic events" and we will discuss them in more detail later in this paper.

The two-pion mass distribution for all events passing the above cuts is shown in Figure 1. The curve shown is a fit to the data of the form:

$$\frac{dN}{dM} = \frac{C_0 M M_p \Gamma}{(M^2 - M_p^2)^2 + M_p^2 \Gamma^2} \left\{ 1 + C_1 \left( \frac{M_p^2}{M^2} - 1 \right) + C_2 \left( \frac{M_p^2}{M^2} - 1 \right)^2 \right\} \epsilon, \quad (2)$$

where  $\Gamma$  is a mass dependent width<sup>5</sup> given by:

$$\Gamma(M) = \left( \frac{q(M)}{q(M_p)} \right)^3 \frac{2\Gamma_0}{1 + [q(M)/q(M_p)]^2},$$

$q(M)$  is the magnitude of the three momentum in the  $\pi^+\pi^-$  center-of-mass frame,  $C_1$ ,  $C_2$  are constants used to parameterize the non-resonant contributions to the dipion mass spectrum, and  $\epsilon$  is the mass dependent geometric acceptance of

our detector as determined from Monte Carlo calculations. The Monte Carlo program generated events with an exponential  $t$ -dependence with slope  $8.5 \text{ GeV}^{-2}$  and a decay angular distribution of  $\sin^2\theta^*$ . The simulation of the response of the recoil detector, Cherenkov counter, and the trigger counters were made based on extensive studies of the behavior of the actual detectors.

In using this form, we follow Spital and Yennie<sup>6</sup> and adopt their convention for defining the  $\rho$  cross-section in terms of the measured dipion cross-section at the  $\rho$  mass. i.e. we define the  $\rho$  yield,  $N_\rho$  as:

$$N_\rho = \frac{\pi}{2} C_0. \quad (3)$$

The best values for the mass  $M_\rho$  and the width  $\Gamma_\rho$  from this fit are:

$$M_\rho = 774 \pm 1 \text{ MeV}$$

$$\Gamma_\rho = 152 \pm 2.5 \text{ MeV.}$$

The mass and width of the  $\rho$  were fixed at these values throughout the rest of the analysis in different energy and  $t$  regions. Only the parameters  $C_0$ ,  $C_1$ , and  $C_2$  were allowed to vary in subsequent fits.

We fit the dipion mass spectrum using the procedure described above in each of 25 photon energy regions covering the range from 45 to 225 GeV. We converted the resulting  $\rho$  yields to cross-sections by dividing by the product of the incident flux with the calorimeter acceptance for each region.

The energy dependence of the incident photon flux was measured by four methods and was documented in a previous paper.<sup>4</sup> The overall normalization was determined by 2 methods: (1) the integrated beam power was measured by a Wilson-type quantameter and corrected for electronic deadtime (34%) and (2) low mass  $e^+e^-$  pairs were collected throughout the data-taking runs using a separate trigger. The total number of incident photons with energy greater

than 45 Gev as determined by each of these methods differed by only 5.5%. The calorimeter acceptance was determined by weighting the observed events by the inverse of the probability that an event with the observed pulse height in the calorimeter would have satisfied the energy deposition requirement. This probability function was determined from data runs in which the energy deposition requirement was  $1/2$  of that in the regular runs. Corrections were also made for each energy region for those events which were not observed because they failed a cut which required the pulse height in the calorimeter to be large enough that the probability for satisfying the energy deposition requirement was greater than 3%.

Additional corrections were made for accidental muon halo vetoes (14%), pion absorption or decay in the spectrometer (7%), misidentification of inelastic events as elastic events by the recoil analysis (4%), and production from the target end caps (3%).

Figure 2 shows our measurements of the elastic  $\rho$  photoproduction cross-section as a function of energy along with the results of some other experiments.<sup>7</sup> Our data is consistent with an energy independent elastic  $\rho$  cross-section of  $10.0 \pm 0.1$  pb. We estimate our overall normalization uncertainty to be  $\pm 7\%$ , with the dominant contribution coming from our knowledge of the incident photon flux ( $\pm 5\%$ ).

To determine the  $t$ -dependence of elastic  $\rho$  photoproduction, we divided our data sample into four energy regions and then for each region fit the dipion mass spectrum using the procedure described above in separate  $t$  bins (11-15 bins) covering the range from 0 to  $1.0$  (Gev/c)<sup>2</sup>. We converted the resulting  $\rho$  yields to differential cross-sections using the Monte Carlo calculations and corrections described previously. In this case, the correction due to production from the target end caps had to be made

t-dependent as we did observe coherent  $\rho$  production from the mylar. The correction for the inelastic contamination was also made t dependent.

Figure 3 shows our measurements of the differential cross-section  $d\sigma/dt$  for elastic  $\rho$  photoproduction as a function of t for each of the four energy regions. The curves in the figure are the result of a one parameter fit of the data to the vector dominance plus additive quark model prediction:<sup>3,9</sup>

$$\frac{d\sigma}{dt} (\gamma + p \rightarrow p + \rho^0) = \frac{4\pi\alpha}{f_\rho} \left( \frac{p_\pi^*}{2p_\gamma} \left( \frac{d\sigma}{dt} (\pi^+ p \rightarrow \pi^+ p) + \frac{d\sigma}{dt} (\pi^- p \rightarrow \pi^- p) \right) \right)^2 \quad (4)$$

where we have taken the t-dependence of elastic  $\pi p$  scattering to be of the form  $A e^{bt + ct^2}$ , where A, b, and c were determined from fits to  $\pi p$  elastic scattering data<sup>8</sup> in the energy region from 50 to 175 Gev. The value determined for the  $\gamma\rho$  coupling constant from the fit is:

$$\frac{f_\rho^2}{4\pi} = 2.39 \pm .02$$

This value is about 10% higher than that determined from an analysis of data from Orsay on the reaction  $e^+e^- \rightarrow \pi^+ + \pi^-$ .<sup>3,10</sup>

We now turn to those events which were eliminated from the elastic analysis only because the information from the recoil detector indicated that the event was not consistent with reaction (1). These "diffractive inelastic" events have similar characteristics to those of the elastic events with the exception of the t-dependence. The "diffractive inelastic" events are more likely to be produced at larger t than are the elastic events. Following the same procedure as before, we fit the dipion mass spectrum in each of 20 t bins for both the elastic and the diffractive inelastic events.

Figure 4 shows the ratio of the diffractive inelastic cross-section to the sum of diffractive inelastic plus elastic cross-section as a function of

t. The curve shown corresponds to the same ratio for  $\pi p$  interactions at 100 Gev,<sup>11</sup> where the diffractive inelastic cross-section is defined as:

$$\frac{d\sigma}{dt}^{\text{inel}} \cong \int_0^{10} dM_x^2 \frac{d^2\sigma}{dt dM_x^2} (\pi^{\pm}_p + \pi^{\pm}_x).$$

The choice of the upper limit of 10 Gev<sup>2</sup> was made to give agreement for the normalization of the predicted curve with our data. The shape of the curve is taken from the  $\pi p$  data with no adjustable parameters. The agreement between our diffractive  $\rho$  photoproduction data and the diffractive  $\pi p$  data is striking and lends new support to the additive quark model.

We wish to thank the staffs of Fermilab and the high-energy group of the University of Illinois for their support and cooperation. We would like to thank Nevis Laboratory for making available to us those parts of the spectrometer which they constructed as well as for the loan of the lead-glass array and Cornell University for the use of a 30D40 analyzing magnet. This research was supported in part by the U.S. Department of Energy.

- (a) Present address: Bell Laboratories, Holmdale, N.J. 07716
- (b) Present address: University of Colorado, Boulder, CO 80309
- (c) Present address: Scientific Applications, Inc., N.W. Bellevue, WA 98021

## References

1. A. R. Erwin, et al., Phys. Rev. Lett. 6, 628 (1961).  
D. Stonehill, et al., Phys. Rev. Lett. 6, 624 (1961).
2. H. R. Crouch Jr. et al., Phys. Rev. Lett. 13, 636 (1964);  
H. R. Crouch Jr. et al., Phys. Rev. Lett. 13, 640 (1964).
3. T. H. Bauer, R. D. Spital, D. R. Yennie, F. M. Pipkin, Rev. Mod. Phys. 50, 261 (1978).
4. M. C. Goodman et al., Phys. Rev. D 22, 537 (1980);  
M. Binkley et al., Phys. Rev. Lett. 48, 73 (1982).
5. J. D. Jackson, Nuovo Cimento 34, 1644 (1964).
6. R. Spital and D. R. Yennie, Nucl. Phys. B106, 269 (1976).
7. R. L. Anderson et al., Phys. Rev. D 1, 27 (1970);  
R. M. Egloff et al., Phys. Rev. Lett. 43, 657 (1979);  
D. Aston, et al., Nucl. Phys. B209, 56 (1982).
8. D. S. Ayres et al., Phys. Rev. D 15, 3105 (1977).
9. H. J. Lipkin, Phys. Rev. Lett. 16, 1015 (1966).

10. V. L. Auslender et al., Sov. J. Nuc. Phys. 9, 69 (1969);  
D. Benaksas et al., Phys. Lett. 839, 289 (1972);  
A. Quenzer, Ph.D. thesis, University of Paris, Sud (1977).
  
11. D. S. Ayres, et al., Phys. Rev. Lett. 37, 1724 (1976).

## Figure Captions

FIG. 1 Two-pion mass distribution for events consistent with the reaction  $\gamma + p \rightarrow \pi^+ + \pi^- + p$ .

FIG. 2 Total cross-section measurements of the reaction  $\gamma + p \rightarrow \rho^0 + p$  as a function of the incident photon energy.

FIG. 3 Measurements of  $d\sigma/dt$  for the reaction  $\gamma + p \rightarrow \rho^0 + p$  as a function of  $t$  for four incident photon energy regions. The shapes and relative intercepts of the curves are constrained to be those found from fits to  $\pi p$  elastic scattering data i.e.  $\frac{d\sigma}{dt} = \frac{\alpha A}{f_\rho^2/4\pi} e^{bt} + ct^2$  where  $f_\rho^2/4\pi = 2.39 \pm .02$ , and

<u>k(Gev)</u>	<u>A(mb/GeV<sup>2</sup>)</u>	<u>b(Gev<sup>-2</sup>)</u>	<u>c(Gev<sup>-4</sup>)</u>
45-75	28.9	9.13	2.49
75-105	28.0	8.92	2.15
105-145	28.7	9.11	2.34
145-225	29.7	9.33	2.58

FIG. 4 Measurements of  $f$ , the ratio of the diffractive inelastic  $\rho$  photoproduction cross-section to the sum of the diffractive inelastic plus elastic  $\rho$  photoproduction cross-sections, as a function of  $t$ . The shape of the curve is constrained to be that found from fits to  $\pi p$  diffractive inelastic and elastic scattering data.

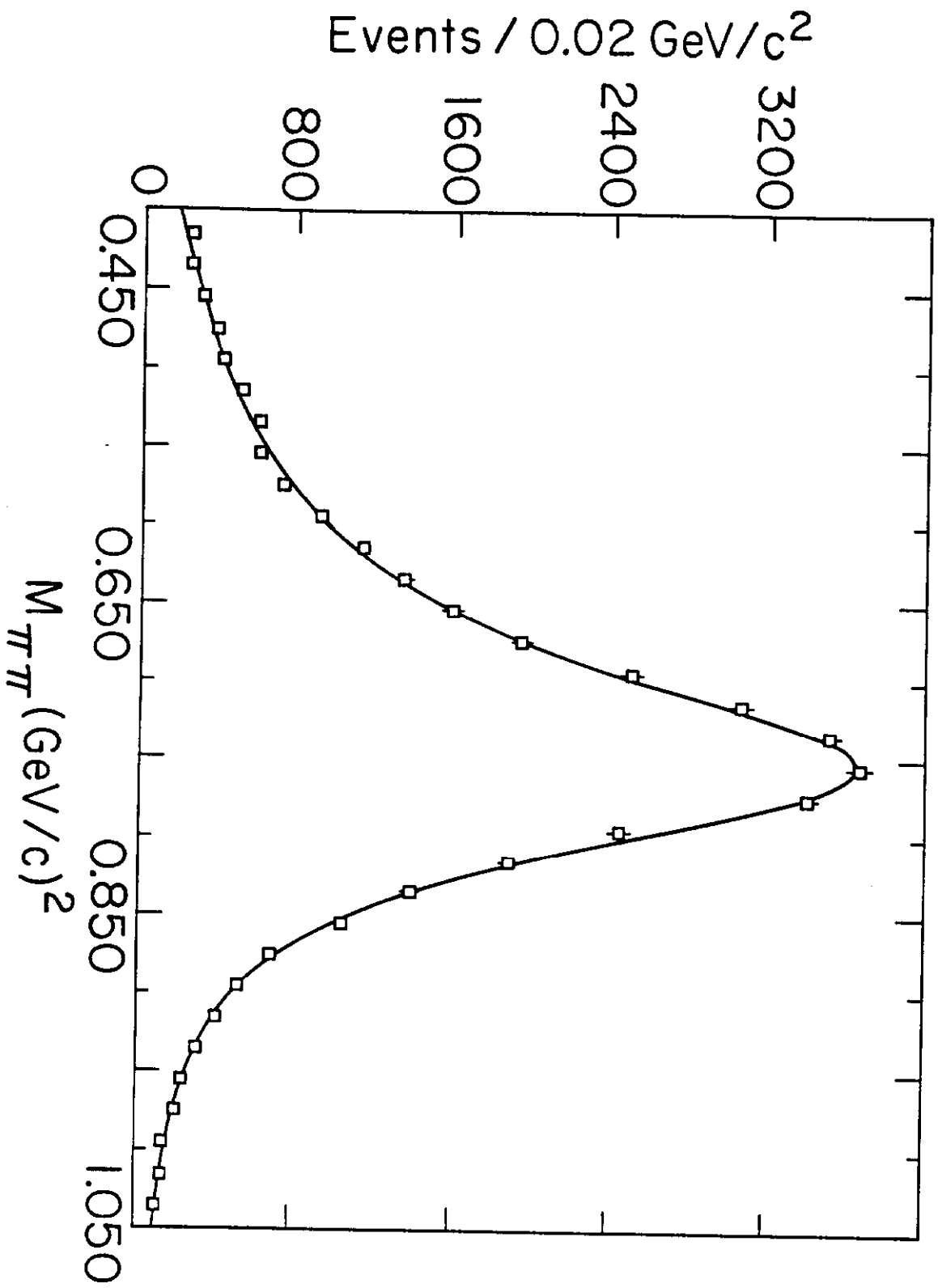


Fig. 1

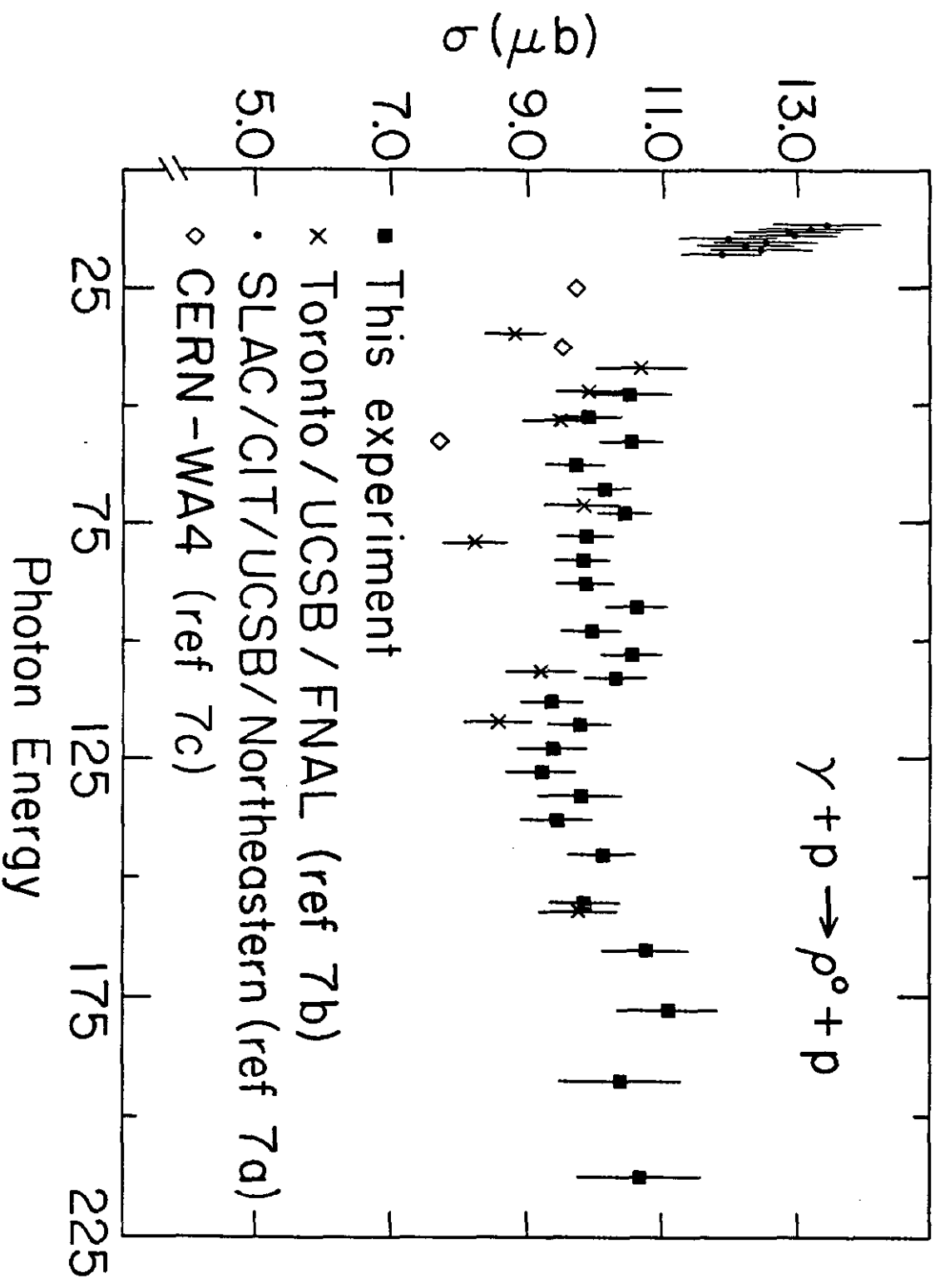


Fig. 2

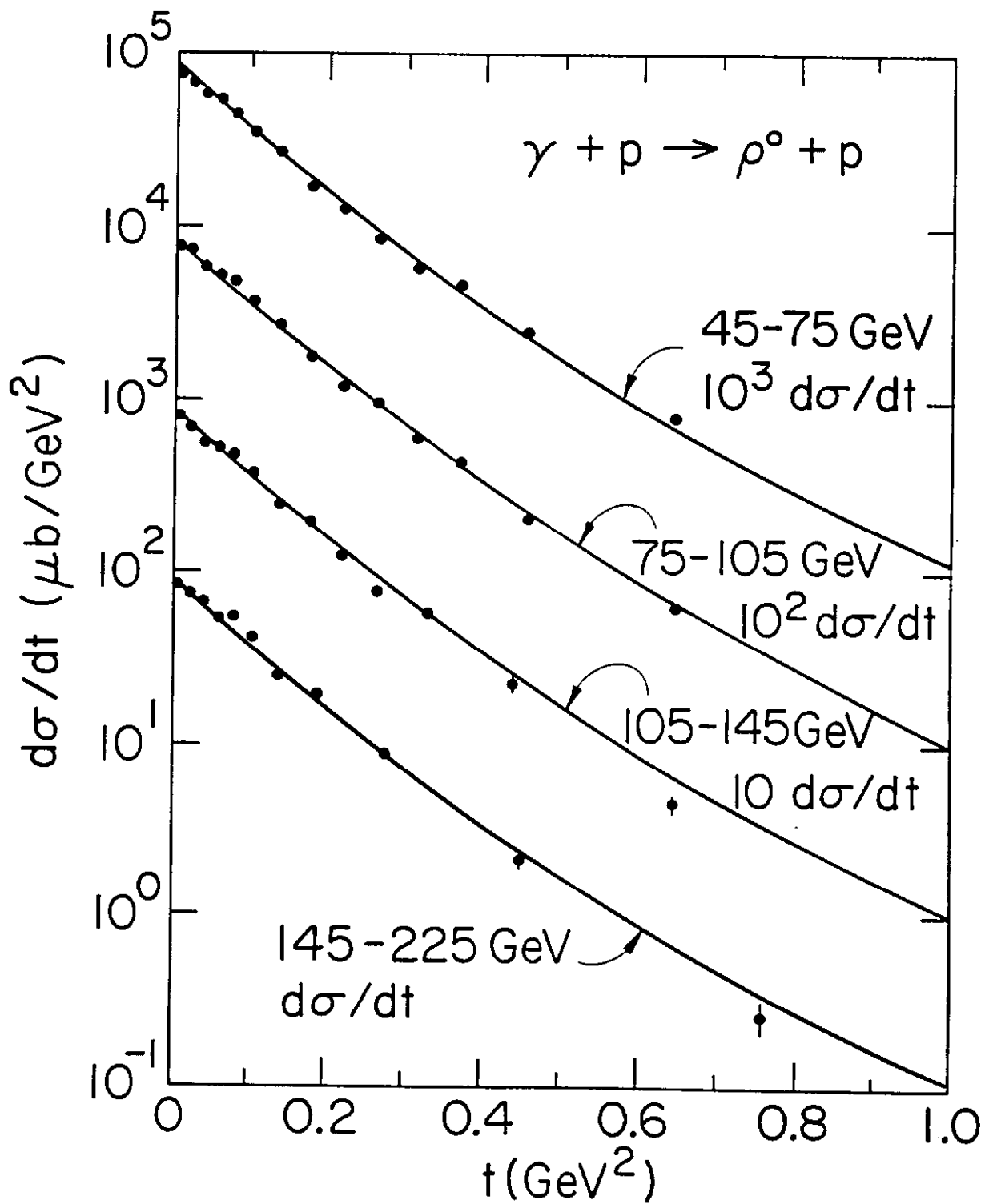


Fig. 3

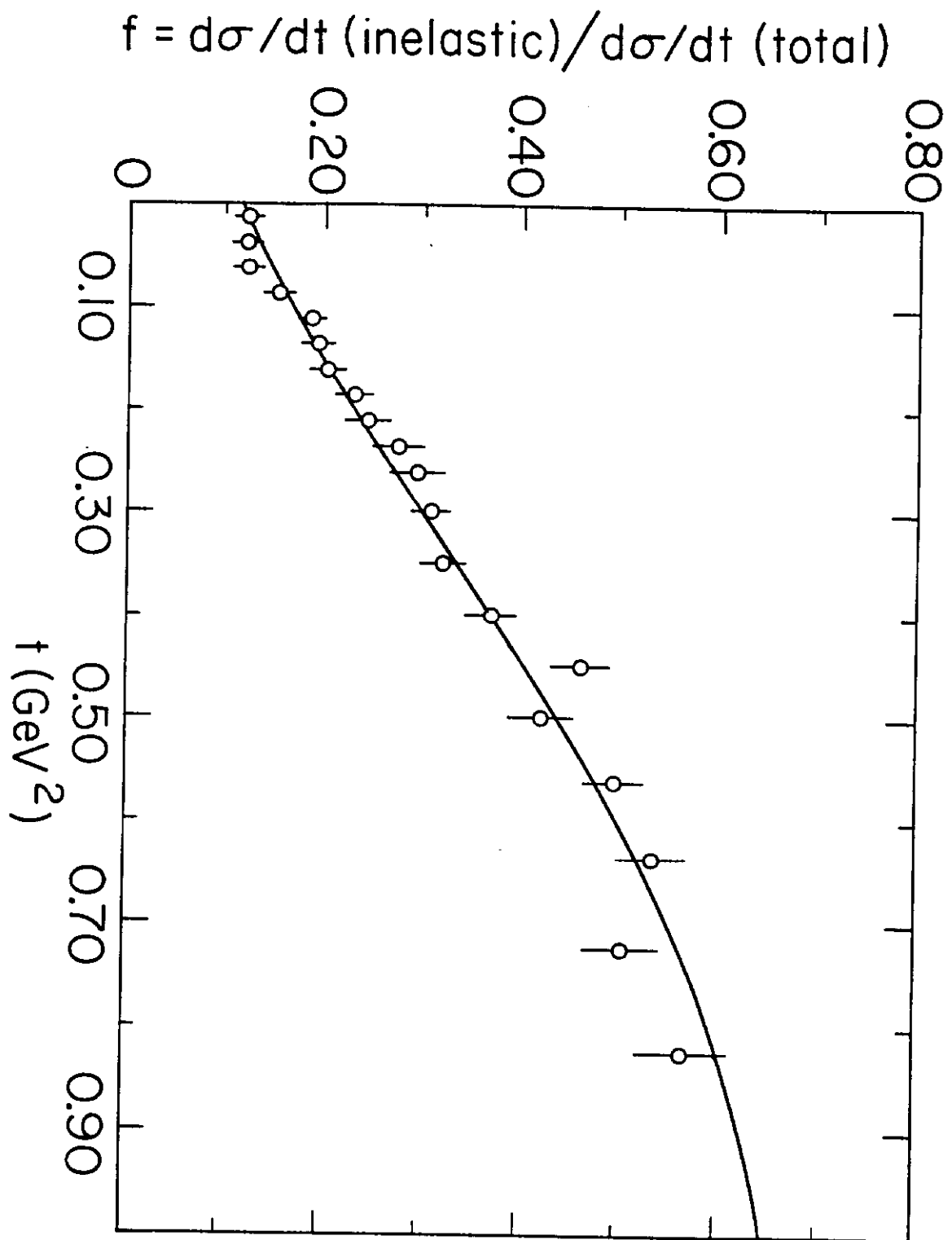


Fig. 4